Aircraft automation principles as a basis for the use of information technologies

Leonid Romaniuk [1,*,†], Marcin Bernas[2,†], Vitalii Kartashov[1,†], Ihor Chykhira[1,†] and Halyna Tulaidan [3,†]

[1] *Ternopil Ivan Puluj National Technical University, 56, Ruska Street, Ternopil 46001,* Ukraine

[2] *University of Bielsko-Biala, Willowa St. 2, Bielsko-Biala, 43-300, Poland*

[3] *Ternopil Volodymyr Hnatiuk National Pedagogical University, 2, Maxyma Kryvonosa Street, Ternopil 46027,* Ukraine

Abstract

Small unmanned aircrafts frequently undergo short-term configuration changes due to their use across a great variety of operational scenarios. For example, special payloads are attached, batteries and screws or other components of modular system are changed. As a result, the boundaries of the flight area are often unknown or uncertain. However, despite these uncertainties, the autonomous unmanned aircraft should be able to follow the controlled trajectory in the limited space. The adaptation of the kinematic motion model for automatic trajectory planning of unmanned aircraft in response to the changing or previously unknown boundaries of the flight area is investigated in this paper. Algorithms for the integration of automatic UA route planning under different conditions, in the presence and absence of obstacles, are proposed. The hypothesis of the investigation is that adequate reference trajectories can be planned simply by determining certain parameters of the kinematic motion model, without additional determination of the reasons of changes within the flight range limits For this purpose, the parameters of the kinematic motion model used for trajectory planning are automatically monitored and updated during the flight. This determination of the model parameters should work without additional devices or additional stimuli from the unmanned aircraft. If the parameter is changed, the reference trajectories are re-planned during flight in accordance with the updated kinematic motion model, so that, on the one hand, the possible sequence of the reference trajectory with limited preservation and restrictions of the available flight area are still used. Subsystems for trajectory planning and for monitoring and determining model parameters are evaluated using simulations and flight test data. The overall system is evaluated by modeling Prometheus unmanned aircraft.

Keywords

Unmanned aircraft, operational scenarios, payload, flight area boundaries, kinematic motion model, autonomous flight, reference trajectory

CITI'2024: 2nd International Workshop on Computer Information Technologies in Industry 4.0, June 12–14, 2024, Ternopil, Ukraine

* Corresponding author.

† These authors contributed equally.

leonidromanyuk@gmail.com (L. Romaniuk); mbernas@ath.bielsko.pl (M. Bernas); kartashov@tntu.edu.ua (V. Kartashov); ig.vi.chi@gmail.com (I. Chykhira); tulaidan@tnpu.edu.ua (H. Tulaidan)

0000-0002-2538-4026 (L. Romaniuk); 0000-0002-0099-1647 (M. Bernas); 0000-0003-0530-3919 (V. Kartashov); 0000-0002-8615-3635 (I. Chykhira); 0000-0003-2306-6435 (H. Tulaidan)

1. Statement of the problem

The ability of autonomous aircrafts to follow trajectories with small spatial trajectory displacements is the requirement for this type of aircraft that should be met in the vast majority of applications, the fulfillment of which ensures that UA does not encounter obstacles, does not violate the boundaries of designated airspace, maintain separation from other air traffic participants, or provide good recordings due to the accurate positioning of the carried sensors, such as cameras. The consequences of insufficient short orbital distances can range from missing mission objectives to safety-critical events such as invasion into undesignated airspace or, especially in the case of low-flying UAs, collision with aircraft obstacles.

2. Analysis of the available investigation results

The idea of reducing complex relationships resulting in the aircraft motion, to a few parameters of the kinematic motion model was formulated in paper [1]. In other words, it was concluded that, in order to create reference trajectories, the parameters of the kinematic motion model should not be derived from the detailed record of measurements of all system and subsystem states or from detailed knowledge of the system. Probably, the idea is that the direct determination of a certain parameters of the kinematic motion model is sufficient for the reference trajectories creation.

In paper [2] the effect of wind speed and direction on UA flight states was investigated, appropriate parameters and methods of their solution under the influence of wind conditions and also the problem of UA logistics route planning, which simultaneously takes into account the UA energy consumption limitations, customer time windows, and the influence of wind conditions were solved. A large-scale neighborhood search (LNS) algorithm was combined with genetic algorithm (GA) creating GA-LNS in order to solve the static problem, while dynamic planning concepts of GA-LNS for solving the dynamic trajectory optimization problem was used in the decoding process. The simulation results show that the developed algorithms reduce the distribution expenses approximately by 9% compared to the ordinary GA.

An optimized route planning algorithm based on the artificial potential field (APF) method was proposed in paper [3]. This method chooses preliminary planning of UA trajectory on the basis of rapidly expanding random tree (RRT). The pre-planned route is divided into continuous parts, and then intermediate route points are created. The route point located nearby generates the gravitational force due to which the UA avoid the local minimum while entering it. At the same time, taking into account the distance from UAV to the obstacle and the radius of influence of the obstacle itself, the gravitational and repulsive coefficients are dynamically adjusted, creating non-gravitational area around the obstacle, which is beneficial for UA to avoid the obstacle.

Sensors are used in the development and operation of autonomous aircraft [4], [5]. An important characteristic of various types of sensors is stability [6], [7]. The implementation of artificial neural networks in the feedback loop in autonomous aircraft improves coordination of movements, accuracy and speed. The article [8] presents the

results of a qualitative study of a neural network, including discrete and distributed time delays. A method for calculating the exponential decay rate for a neural network model based on differential equations with a discrete delay was developed and applied [9], [10]. Numerical modeling in cyber-physical sensor systems [11], [12] for automated control of autonomous aircraft is important at the stage of their design.

3. Statement of the task

Accurate trajectory planning requires information about the kinematic or dynamic model of unmanned aircraft motion for its proper trajectory planning. In this paper, kinematic model of Dubins' aircraft motion is used for reference trajectory planning. The reference trajectories that are planned using the Dubins motion model are described in detail for the vast majority of mission scenarios, including obstacle settings, and the application of this motion model is particularly suitable for efficient in-flight trajectory planning.

For unmanned aircrafts, reference trajectories can be created by determining the kinematic model parameters during nominal flight over rough terrain and adaptive trajectory planning by means of the model of the Dubins aircraft motion with static wind, even if the parameters of the kinematic model are known with errors only in advance.

Since aircraft movements similar to those of the Dubins automobile model occur in three-dimensional space, the model was extended to three-dimensional configuration as shown in Equation 1. The route velocity $\vec{V}_K = (u_k, v_k, w_k)^T$ is parameterized according to time t and is described as follows:

$$u_k(t) = V_k \cos(\dot{\chi} \cdot t + \chi_0) \cos(\gamma) \tag{1a}$$

$$v_k(t) = V_k \cos(\dot{\chi} \cdot t + \chi_0) \cos(\gamma) \tag{1b}$$

$$w_k(t) = V_k \sin(\gamma) \tag{1c}$$

where v_k is the value of route speed, $\dot{\chi}$ is the change of orbital azimuth, χ_0 is the initial orbital azimuth and γ is the trajectory angle. It is assumed that $v_k = {}^{m}/_{s^2}$. Using this model, the flight trajectory can be modeled in sections in straight and curved flight $\dot{\chi} \in \{-\dot{\chi}\,\max, 0, \dot{\chi}\,\max\}$, as well as in horizontal flight, climb or descent $\gamma \in \{-\gamma\,\max, 0, \gamma\,\max\}$. The model equations can be integrated analytically by closed segments in time. With the time parameter τ and $\vec{x}_g(t) = \int_0^t \vec{V}_k(\tau)d\tau$ in forward flight τi $\vec{x}_g(t) = \int_0^t \vec{V}_k(\tau)d\tau$, the following is applied

$$x_g(t) = V_k \cos(\chi_0) \cos(\gamma) \cdot t + x_0 \tag{2a}$$

$$y_g(t) = V_k \sin(\chi_0) \cos(\gamma) \cdot t + y_0 \tag{2b}$$

$$z_g(t) = V_k \sin(\gamma) \cdot t + z_0 \tag{2c}$$

with the initial position $\vec{x}_0 = (x_0, y_0, z_0)^T$ at the moment of time $t_0 = 0\,s$ and the initial azimuthal angle of orbit χ_0. At turn $\chi \neq 0$, the result is as follows:

$$x_g(t) = \frac{V_k}{\dot{\chi}} \sin(\dot{\chi} \cdot t + \chi_0) \cos(\gamma) + x_0 - \frac{V_k}{\dot{\chi}} \sin(\chi_0) \cos(\gamma) \tag{3a}$$

$$y_g(t) = \frac{V_k}{\dot{\chi}} \cos(\dot{\chi} \cdot t + \chi_0) \cos(\gamma) + y_0 - \frac{V_k}{\dot{\chi}} \cos(\chi_0) \cos(\gamma) \tag{3b}$$

$$z_g(t) = V_k \, sin(\gamma) \cdot t + z_0 \tag{3c}$$

In case of $\gamma = 0$, the following applies to the resulting radius of the curve R:

$$R = \frac{V_k}{\dot{\chi}} \tag{4}$$

Examples of trajectories according to equations (2) and (3) are shown in Figure 1. The horizontal trajectory shown in Figure 1a consists of two straight segments and one circular curve. Transitions between straight and turning flight are modeled by sudden changes in the azimuth and angle χ of the trajectory. These sudden changes are the approximation to the real UA motion. The boundaries of the segments are marked with dashed lines.

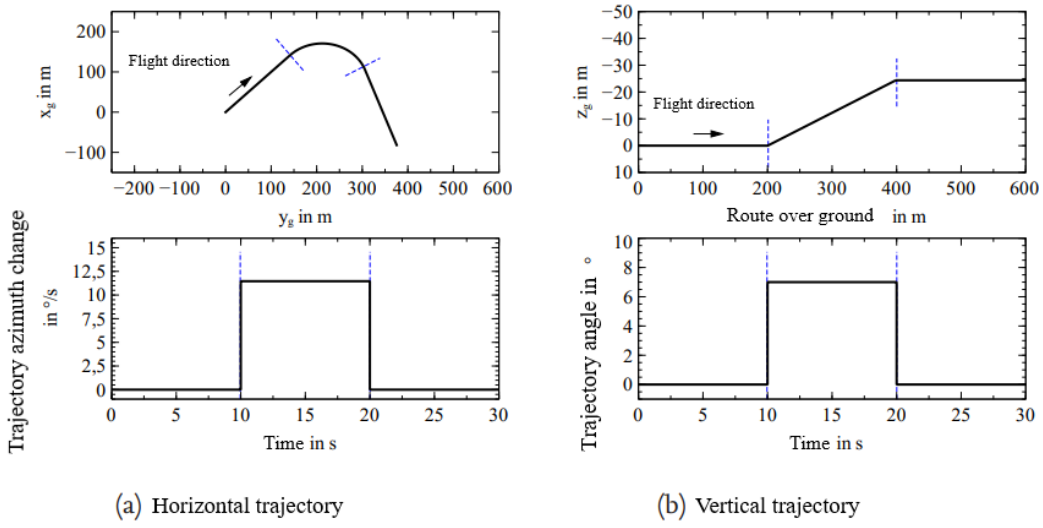

Figure 1: Example of aircraft motion according to the Dubins' aircraft motion model

The vertical trajectory shown in Figure 1b is the climb segment. The transitions between horizontal flight and climb or descent are modeled by sudden changes in the trajectory angle γ. This is also the approximation of UA motion model. Changes in the trajectory speed $V_k$will be modeled as the approximation through sudden changes in V_k. as well. While the Dubins aircraft motion model just roughly describes the motion of the real

aircraft at segment transitions, the simulated segment motion corresponds to the real motion of the aircraft in the stationary flight.

Aircraft motion is modeled by the Dubins airplane motion model with the parameters of the the angle of inclination of the flight wind γ_A and turn speed $\dot{\Psi}$. Limitations of flight characteristics are described by $\gamma_{A,max}$ and $\dot{\Psi}_{max}$., respectively. Another general representation of the UA flight and technical characteristics under stationary flight conditions is the description of the permissible values of the lift force coefficient C_A, propulsion system power P, and multiple load n[13].

The following assumptions are used to consider stationary flight conditions. The stationary flight is described by the balance of forces and moments and coordinated turning flight is assumed, i.e., the sliding angle $\beta = 0$ and lateral force are zero. In addition, it is supposed that there is no wind and the thrust vector is located along the UA longitudinal axis. With centripetal force acting on the UA during turn $F_{zp} = V_A^2 \cos^2 \gamma / R$, with curve radius R the balance of forces and moments along the fixed orbit coordinate system (x_k , y_k , z_k) will be as follows:

$$\sum F_{xk} = 0 = D - T\cos\alpha + G\sin\gamma \tag{5a}$$

$$\sum F_{yk} = 0 = \frac{G}{8}\frac{V_A^2 \cos^2\gamma}{R} - A\sin\Phi + T\sin\alpha\sin\Phi \tag{5b}$$

$$\sum F_{zk} = 0 = A\cos\Phi + T\sin\alpha\cos\Phi - G\cos\gamma \tag{5c}$$

$$\sum M_{xk} = 0 \tag{5d}$$

$$\sum M_{yk} = 0 \tag{5e}$$

$$\sum M_{zk} = 0 \tag{5f}$$

In equations 5, A is the lifting force, D is the resistance force, g = m • g is the gravity force, T is the traction force, α is the angle of attack, , $g \approx 9{,}81$ m/s is the gravitational acceleration, Φ is the overhang angle, and γ is the trajectory angle. For small angles of attack α, it is further assumed that $\cos\alpha \approx 1$ and $\sin\alpha \approx 0$. The result of the force balance is as follows:

$$\sum F_{xk} = 0 = D - T + G\sin\gamma \tag{6a}$$

$$\sum F_{yk} = 0 = \frac{G}{8}\frac{V_A^2 \cos^2\gamma}{R} - A\sin\Phi \tag{6b}$$

$$\sum F_{zk} = 0 = A\cos\Phi + W\cos\gamma \tag{6c}$$

The ratio is valid at a constant flight speed and horizontal flight without sliding

$$\dot{\Psi} = \frac{g \cdot \tan\Phi}{V_A} \tag{7}$$

between the angle of overhang Φ and turning speed Ψ̇ with the gravity acceleration g.

The UA environment is described by the state space s X and states x ∈ X. In this state space, it is required for agent A to plan its motion from state $x_s \in X$ to state $x_z \in X$ or into the state space $x_Z \subset X$. Agent A can move within its action space U with actions u ∈ U in the space states. For the motion in state space, the function of transition f from state x to the new state ẋ is given in the form of the state transition equation:

$$\dot{x} = f(x, u) \tag{8}$$

Similarly, the transition equation is given in time-discretized representation

$$x_{t+1} = f(x_t, u_t) \tag{9}$$

For the actual planning, the state space is transferred to the configuration space C with the configurations q ∈ C that are relevant for planning. The allowable configuration space is limited by the interference region C_{obs}. Space C_{obs} is often artificially enlarged in order to ensure the absence of obstacle between agent A and the actual obstacle. In the remaining free space $C_{free} = C/C_{obs}$, agent A is able to move according to its action space U. Similar to equation (8), the transition equation in configuration space is $\dot{q} = f(q, u)$.

Thus, the planning algorithm should be able to create continuous route τ: [0,1] → for agent A from the initial configuration $q_S \in C_{free}$ to the target configuration $q_Z \in C_{free}$ or $C_Z \in C_{free}$ з $\tau(0) = q_S$ і $\tau(1) = q_Z$ or report correctly that this route does not exist. If these properties are true, the planning algorithm is considered to be complete. Very often the cost function g is also defined in such a way that the planning algorithm returns the optimal route regarding the cost function.

Automatic route planning calculates the reference trajectories for cruise flight by UA motion model. By means of appropriate reference route, route deviation occurring during the route sequence can be minimized. While selecting the appropriate algorithm for route planning against the background of obstacles, it is recommended to use sampling-based approaches, as the obstacle background can be effectively taken into account by discretizing the planning space depending on the method complexity.

PRM trajectory planning approaches that use kinematic motion model have been presented for UA trajectory planning. These approaches use local motion planning in accordance with the Dubins model of aircraft motion with curve straight curve (CSC) segments and the cyclic search graph with cyclic search graph with search on the graph in order to find the optimal reference trajectory according to the cost functionality. The calculation of SCS trajectory segments makes it possible to solve efficiently the problem of

motion planning and results in reference routes where straight and curved segments always alternate. Compared to planing by CSC segments, direct transitions between two curves in opposite directions, which in the case of the airplane mean maximum sudden changes in the overhang angle, are avoided. However, while selecting SCS segments for the solution of motion planning in space without obstacles, the methods of trajectory planning in obstacle conditions should be adapted and cannot be adopted from existing approaches without modification. Eventually, the choice of local planning problem ensures sequential movement of complex calculation steps to the initialization phase and less complex calculation steps to the time-critical planning phase. In addition to the initial and target states (q_S, q_Z), the division makes it possible to set up the planning parameters $(\dot{\Psi}_p, \gamma_{A,p}, V_{W,p}, \chi_{W,p}, S_p)$ for each planning request and simultaneously the time to achieve effective planning.

Applying the transition functions or equations of the Dubins aircraft motion model and trajectory planning parameters $\dot{\Psi}_p, \gamma_{A,p}, V_{W,p}, \chi_{W,p}$, the segmental reference trajectories for aircraft $\vec{x}_p(t)$ can be calculated with fixed wing in space without obstacles C_{free} in the fixed Earth coordinate system:

$$\vec{x}_p(t) = \int_0^t \vec{x}_p(\tau) d_\tau + \vec{x}_{p0} \tag{10}$$

In equation (10), $\vec{x}_p$ corresponds to the motion, t and τ to time, and $\vec{x}_{p0}$ to the initial position at time $t = 0$.

Further, we consider the problem of planning the transition between two intersecting lines and give the calculation rule for solving the planning problem. The transition between the two intersecting lines is simulated by means of the curve, resulting in SCS segment formation. The premise is that two linear flight segments [AB] and [BC] intersect at point B, as shown in Figure 2. In this case.

$$\vec{x}_{AB}(t) = \vec{A} + \vec{V}_{K,A} \cdot t \tag{11}$$

describes the initial segment [AB] with fixed relative to the Earth velocity $\vec{V}_{K,A}$ at point A, while in

$$\vec{x}_{BC}(t) = \vec{C} + \vec{V}_{K,C} \cdot t \tag{12}$$

the target segment [BC] with fixed relative to the Earth velocity $\vec{V}_{K,C}$ at point C is described. In addition, condition $\Delta\chi < 180^\circ$ should be applied to the change of the azimuth of the angle trajectory $\Delta\chi := 180^\circ - \angle ABC$. The condition for intersection of segments [AB] and [BC] isas follows:

$$\vec{A} + \vec{V}_{K,A} \cdot t_A = \vec{C} + \vec{V}_{K,C} \cdot t_C \text{ з } t_A, t_C \geq 0 \tag{13}$$

Below, we describe The determination of the transition times t_1, t_2, t_3 between the straight and curved segments shown in Figure 2 are described and calculation of the

reference trajectory with SCS segment, taking into account the Dubins aircraft motion model is presented.

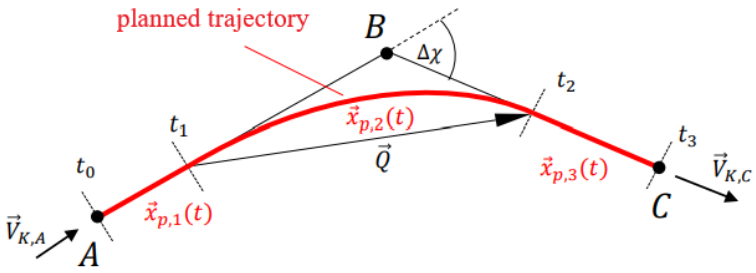

Figure 2: The straight-curve-straight planning problem in the obstacle-free space

First, the normalized air speed vector for two linear flight segments at points A and C is calculated. The value of the flight speed V_A, wind speed $\vec{V}_W$ and direction of the orbital velocity vector $\vec{V}_{K,n}$ are given:

$$V_K = \vec{V}_{K,n} \cdot \vec{V}_W + \sqrt{(\vec{V}_{K,n} \cdot \vec{V}_W)^2 - V_w^2 + V_A^2} \tag{14}$$

$$\vec{V}_{A,A} = \frac{1}{V_A} \cdot (V_K \cdot \vec{V}_{K,n} - \vec{V}_W) \tag{15}$$

With known air speed vectors, azimuth Ψ_1 i Ψ_3 for segments $\vec{x}_{p,1}(t), \vec{x}_{p,2}(t)$ and the change in azimuth $\Delta\Psi = |\Psi 3 - \Psi 1|$ can be defined. For special case $\Delta\Psi = 0^{\circ}$ the reference route is the result of two linear segments [AB] and [BC].

Time $\Delta t_{1,2} = t_2 - t_1$ for curve segment $\vec{x}_{p,2}(t)$ is defined now as:

$$\Delta t_{1,2} = \frac{\Delta\Psi}{|\dot{\Psi}_p|} \tag{16}$$

With known $\Delta t_{1,2}$, the endpoint for $\vec{x}_{p,2}(\Delta t_{1,2})$ can be determined by equations (3) and initial values $x_0 = 0, y_0 = 0, \Psi_0 = \Psi_1$. It is defined as the position vector $\vec{Q} := \vec{x}(\Delta t_{1,2})$.

Now the curve segment is known up to the actual starting point $\vec{x}_{p,1}(t_1) = \vec{x}_{p,1}(\Delta t_{0,1})$ since $t_0 = 0$ s. Points $\vec{x}_{p,1}(t_1)$ i $\vec{x}_{p,2}(t_2)$ can be found by the system of linear equations in the horizontal plane, which can be expressed in the following way:

$$\vec{C} = \vec{A} + \Delta\vec{x}_{p,1} + \vec{Q} + \Delta\vec{x}_{p,3} \tag{17a}$$

$$\vec{C} - \vec{A} = \vec{V}_{K,A} \cdot \Delta t_{0,1} + \vec{Q} + \vec{V}_{K,C} \cdot \Delta t_{2,3} \tag{17b}$$

$$\vec{C} - \vec{A} - \vec{Q} = \vec{V}_{K,A} \cdot \Delta t_{0,1} + \vec{V}_{K,C} \cdot \Delta t_{2,3} \tag{17c}$$

and can be solved for two unknown values $\Delta t_{0,1}$ i $\Delta t_{2,3}$. Then the transition time results in:

$$t_0 = 0, \tag{18}$$

$$t_1 = \Delta t_{0,1}, \tag{19}$$

$$t_{21} = t_1 + \frac{\Delta t_{1,2}}{2}, \tag{20}$$

$$t_{22} = t_{21} + \frac{\Delta t_{1,2}}{2}, \tag{21}$$

$$t_3 = t_{22} + \Delta t_{2,3} \tag{22}$$

In this case, the following condition should be applied: $t_0 \leq t_1 \leq t_{21} \leq t_{22} \leq t_3$.

Now the complete reference trajectory parameterized according to time t is known. The second segment s_2 is divided by the change of the inclination angle of the flight wind into $\vec{x}_{p,21}$ i $\vec{x}_{p,22}$. If points A,B,C are located on the straight line, then $\vec{x}_{p,2}$ is descended, since $t_1 = t_{21} = t_{22}$. In the general case, the SCS route segment $\vec{x}_p(t), t \in (0, t_3)$ results in:

$$\vec{x}_{p,1}(t) = \vec{A} + t \cdot \vec{V}_{K,A}, \quad t \in (0, t_1], \quad \dot{\Psi}_p = 0, \gamma_{A,p} = \gamma_1 \tag{23a}$$

$$\vec{x}_{p,21}(t) = \vec{x}_{p,1}(t) + \vec{x}(t), \quad t \in (t_1, t_{21}], \quad \dot{\Psi}_p \neq 0, \gamma_{A,p} = \gamma_1 \tag{23b}$$

$$\vec{x}_{p,22}(t) = \vec{x}_{p,21}(t) + \vec{x}(t), \quad t \in (t_{21}, t_{22}], \quad \dot{\Psi}_p \neq 0, \gamma_{A,p} = \gamma_3 \tag{23c}$$

$$\vec{x}_{p,3}(t) = \vec{x}_{p,22}(t) + t \cdot \vec{V}_{K,C}, \quad t \in (t_{22}, t_3], \quad \dot{\Psi}_p = 0, \gamma_{A,p} = \gamma_3 \tag{23d}$$

For cases $\gamma_1 > 0 \wedge \gamma_3 > 0 \wedge \dot{\Psi}_p \neq 0$ and $\gamma_1 < 0 \wedge \gamma_3 < 0 \wedge \dot{\Psi}_p \neq 0$ there is the sudden change point in the vertical course. If this discontinuity is not desirable, the transition can be smoothed, for example, by means of polynomial as stated in paper [19] or the entire vertical profile can be smoothed using double integrator as in paper [20].

4. Main results

While planning motion only in obstacle-free space, in addition to the route segments by specifying reference points A, B, C, complete reference routes can also be planned in obstacle-free space. For this paper, the calculation rule was implemented in C++ programming language.

For clarifying reference points A1, B1, C1 for SCS segment are drawn in Figure 3a. The complete reference route consists of four SCS segments. In order to illustrate the influence of wind, the reference trajectory of the motion pattern for $V_A = 20\frac{m}{s}, \dot{\Psi}_p = 0{,}85$ rad/s

without and with wind $V_{W,p} = 6$ m/s is shown. Transitions between separate straight and curved route segments are shown by dotted lines. Comparing two reference trajectories, one can clearly see the consideration of static wind during the trochoid-shaped curve segments in Figure 3b.

z

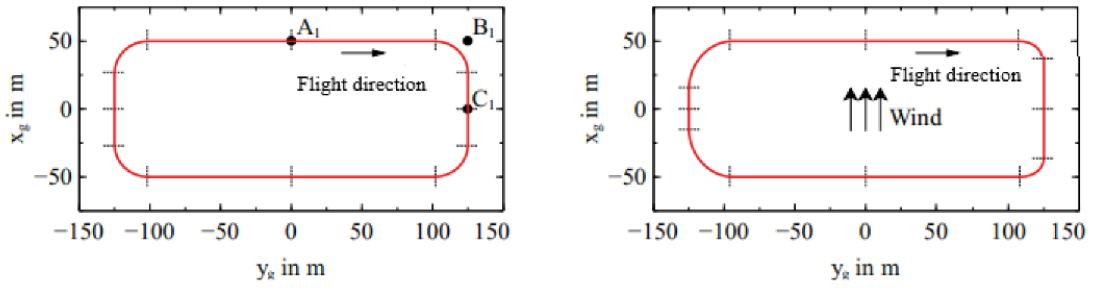

(a) Traffic pattern without wind influence (b) Traffic pattern with wind influence

Figure 3: Examples of trajectories according to the Dubins aircraft motion model with static wind.

$V_A = 25$ m/s i $\dot{\Psi}_p = 0{,}167$ rad/s are accepted for planning. The flight altitude is constant and equals 100 m, and the reference trajectory describes the flight with planned flight time of about 18 minutes.

Calculation times of separate motion planning segments for the implemented SCS motion planning algorithm on the desktop and on-board computers are shown in Table 1. Calculation time for CSC motion planning with the Dubins aircraft motion model with static wind and calculation time for simple straight-straight–SS route planning are shown for comparison,.

Table 1

Calculation results of separate motion planning segments for the implemented SCS motion planning algorithm on the desktop and on-board computers

Individual motion planning	Desktop PC results in ms	On-board computer results in ms
SCS($V_{W,p} = 0$m/s)	0.01	0.03
SCS($V_{W,p} \neq 0$m/s)	0.07	0.22
SS ($\Delta\chi$=0°)	0.00004	0.0002
CSC($V_{W,p} \neq 0$m/s)	0.44	1.96

After the development of the UAV motion planning algorithm, it is requered to carry out the experimental scenario, shown schematically in Figure 4. The UA should fly around the right shaded obstacle, passing through the gap between the obstacles. Static obstacle height $S_{stat} = 10$ m. is initially assumed for route planning. The expected route deviations are initially taken as the expected dynamic route displacement of $S_{dyn} = 15$ m. Thus, the

initial baseline trajectory in Figure 4a is planned with the obstacles height of $S_p = 25$ m. However, after the start of the mission, lateral deviations of the trajectory $d_{y,max} = 41{,}5$ m occur on the first curve. These route deviations are taken into account in path planning as $S_{dyn} = 41{,}5$ m ($S_p = 51{,}5$ m) at the moment of base route replanning. It means that taking into account adaptive obstacle clearance, the route planning excludes passage between obstacles and plans detours. The resulting reference trajectory does not create the risk of breaking the static distance S_{stat} from obstacles or even collision.

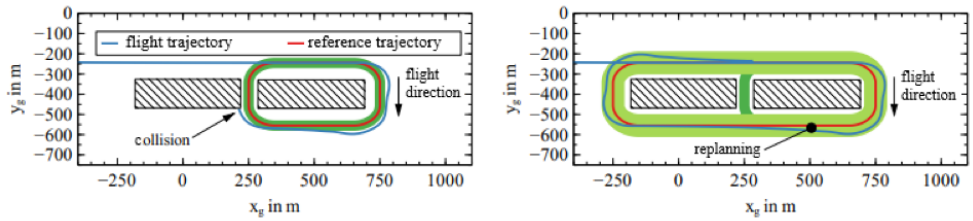

(a) Path course without replanning, with violation of obstacle clearance as a result of lateral path deflections

(b) Path course with replanning

Figure 4: Adaptation of obstacle clearance as the result of lateral route deviations

Automatic trajectory planning using the Dubins parametrized aircraft motion model with static wind is effective due to the application of constant cyclic graphs. The local problem of planning SCS motion in space without obstacles and representing the available free space on the graph structure is proposed fo the approachThis devision makes it possible to carry out intensive computations at one-time initialization stage and to perform only efficient computations at the planning stage.

The presented approach for route planning solves the problem of route smoothing after route planning, which is related to the question how the actual curve radii of the aircraft can be taken into account during planning and not only during the trajectory smoothing. In this investigation, The local motion planning during search on the graph is solved and virtual dual graph is introduced in this investigation.

In case when we take into account the span of obstacles, information about maximum spatial trajectory reached at the moment of flight is used. The assessment shows how obstacles that have already been encountered can be taken into account when planning their overcoming. Since the trajectory deviations resulting from incorrect parameterization of flight characteristics can be accumulated, the obstacle clearance adaptation is less suitable for consideration of incorrect parameterization of flight characteristics. The resulting trajectory deviations are not affected by the obstacle clearance adaptation.

The proposed method defines the trajectory planning parameterization due to which unmanned aericraft can follow the planned reference trajectories close to the limits of flight characteristics. If the increase of safety level is required, the distance from obstacles can be adjusted by the static obstacle distance S_{stat}. Knowing the expected trajectory

positions due to uncertain wind estimate, the distance from obstacles can be regulated as well.

Conclusions

The implementation of autonomous trajectory planning is a basic requirement for various operational scenarios for unmanned aircrafts. Due to the Dubins motion model combined with SCS trajectory planning algorithm, a reliable framework for efficient UA navigation in complex environments was created.

The Dubins motion model offers a simplified approach to the fixation of motion kinematics of UAV movement, making it possible to plan the trajectory accurately taking into account the such limitations as minimum turning radius and maximum speed. Integrating this model with SCS trajectory planning algorithm, which optimizes trajectories based on spatial constraints and mission objectives, it is possible to obtain synergistic interaction that increases the autonomy and adaptability of operations involving direct UA participation. In general, the presented method of adaptive trajectory planning represents the system that can relieve the workload of the ground station operator by adapting automatically the trajectory planning parameters and contributes to the increased autonomy of unmanned aircraft.

References

[1] Ducard G., Kulling K., Geering H.A Simple and Adaptive On-Line Path Planning System for a UA. Control & Automation, 2007. MED'07. Mediterranean Conference on. IEEE. Athens, Greece, June 2007. P. 1–6.

[2] Pengfei D., Yueqiang S., Haotong C, Sahil G., Mubarak A., Piyush S. AI-Enabled Trajectory Optimization of Logistics UAVs With Wind Impacts in Smart Cities. IEEE Transactions on Consumer Electronics. 2024. PP. 1-1.

[3] Xinyi L. Improved path planning method for unmanned aerial vehicles based on artificial potential field. Applied and Computational Engineering. 2023.

[4] Butt M., Nasir N., Rashid R. A. A review of perception sensors, techniques, and hardware architectures for autonomous low-altitude UAVs in non-cooperative local obstacle avoidance. In Robotics and Autonomous Systems. 2024. Vol. 173, p. 104629.

[5] O. Lypak, V. Lytvyn, O. Lozynska, R. Vovnyanka, Y. Bolyubash, A. Rzheuskyi, et al., "Formation of Efficient Pipeline Operation Procedures Based on Ontological Approach", Advances in Intelligent Systems and Computing III: Selected Papers from the International Conference on Computer Science and Information Technologies CSIT 2018, pp. 571-581, September 11-14, 2018

[6] Sverstiuk A. Research of global attractability of solutions and stability of the immunosensor model using difference equations on the hexagonal lattice. Innovative Biosystems and Bioengineering. 2019. Vol. 3 (1), pp. 17 – 26.

[7] Martsenyuk V., Sverstiuk A., Andrushchak I. Approach to the study of global asymptotic stability of lattice differential equations with delay for modeling of immunosensors. Journal of Automation and Information Sciences. 2019. Vol. 51 (2), pp. 58 – 71.

[8] Martsenyuk V., Andrushchak I., Sverstiuk A., Klos-Witkowska A. On investigation of stability and bifurcation of neural network with discrete and distributed delays.) Lecture Notes in Computer Science (including subseries Lecture Notes in Artificial Intelligence and Lecture Notes in Bioinformatics). 2018. Vol. 11127. Pp. 300 – 313.
[9] Martsenyuk V., Sverstiuk A. An exponential evaluation for recurrent neural network with discrete delays. System Research and Information Technologies, 2019. Vol. 2. pp. 83 – 93.
[10] Nakonechnyi O., Martsenyuk V., Sverstiuk A. On Application of Kertesz Method for Exponential Estimation of Neural Network Model with Discrete Delays. Mechanisms and Machine Science. 2020. Vol. 70. pp. 165 – 176.
[11] Martsenyuk V., Sverstiuk A., Klos-Witkowska A., Nataliia K., Bagriy-Zayats O., Zubenko I. Numerical analysis of results simulation of cyber-physical biosensor systems. CEUR Workshop Proceedings. 2019. Vol. 2516, pp. 149 – 164.
[12] Martsenyuk V., Sverstiuk A., Bahrii-Zaiats O., Kłos-Witkowska A. Qualitative and Quantitative Comparative Analysis of Results of Numerical Simulation of Cyber-Physical Biosensor Systems. CEUR Workshop Proceedings. 2022. Vol. 3309, pp. 134 – 149.
[13] Romaniuk L., Chykhira I. Aerodynamic model of a group of uavs in aircraft space. COMPUTER-INTEGRATED TECHNOLOGIES: EDUCATION, SCIENCE, PRODUCTION. Lutsk, 2020, No. 38, P. 59-66.
[14] Romaniuk L., Chykhira I. Automated airtraffic control system of unmanned aerial vehicles. Scientific notes of Taurida National V.I. Vernadsky University. Series: Technical Sciences. Kyiv, 2020. Vol.31. (70). P. 131-135.
[15] Romaniuk L., Chykhira I. Mechanism of ensuringsafe UAV movement under the condit ions of radioattacks: Array. Municipal economy of cities, 2020, Vol. 4, No. 157, P. 178–183.
[16] Romaniuk L., Chykhira I., Tulaidan H., Mykytyshyn A. Model of motion route of unmanned aerial vehicles operations with obstacles avoidance. ICAAEIT 2021, 15-17 December 2021. P. 193–199.
[17] Romaniuk L., Chykhira I., Kartashov V., Dombrovskyi I. UAV movement planning in mountainous terrain. Scientific Journal of TNTU, 2023. Vol 110. No 2. Pp. 15–22.
[18] Xu X., Wang M., Mao Y. Path planning of mobile robot based on improved artificial potential field method. Journal of Computer Applications. 2020 №40(12). P. 3508.
[19] Benders S. Reconfigurable Path Planning for Fixed-Wing Umanned Aircraft Using Free-Space Roadmaps. International Conference on Unmanned Aircraft Systems (ICUAS). IEEE. Dallas, TX, USA, June 2018. P. 891–898.
[20] Schopferer S., Pfeifer T. Performance-Aware Flight Path Planning for Unmanned Aircraft in Uniform Wind Fields. International Conference on Unmanned Aircraft Systems (ICUAS). IEEE. Denver, CO, USA, June 2015. P. 1138–1147.